Search for doubly charmed baryons and study of charmed strange baryons at Belle

Y. Kato,[36] T. Iijima,[37,36] I. Adachi,[11] H. Aihara,[62] D. M. Asner,[47] T. Aushev,[20] A. M. Bakich,[56] A. Bala,[48] Y. Ban,[49] V. Bhardwaj,[38] B. Bhuyan,[14] A. Bobrov,[3] G. Bonvicini,[68] A. Bozek,[42] M. Bračko,[31,21] T. E. Browder,[10] D. Červenkov,[4] V. Chekelian,[32] A. Chen,[39] B. G. Cheon,[9] K. Chilikin,[20] R. Chistov,[20] K. Cho,[24] V. Chobanova,[32] Y. Choi,[55] D. Cinabro,[68] J. Dalseno,[32,58] M. Danilov,[20,34] Z. Doležal,[4] Z. Drásal,[4] A. Drutskoy,[20,34] D. Dutta,[14] K. Dutta,[14] S. Eidelman,[3] H. Farhat,[68] J. E. Fast,[47] T. Ferber,[6] V. Gaur,[57] N. Gabyshev,[3] S. Ganguly,[68] A. Garmash,[3] R. Gillard,[68] Y. M. Goh,[9] B. Golob,[29,21] J. Haba,[11] K. Hayasaka,[37] H. Hayashii,[38] X. H. He,[49] Y. Horii,[37] Y. Hoshi,[60] W.-S. Hou,[41] Y. B. Hsiung,[41] K. Inami,[36] A. Ishikawa,[61] Y. Iwasaki,[11] T. Iwashita,[38] I. Jaegle,[10] T. Julius,[33] J. H. Kang,[70] E. Kato,[61] T. Kawasaki,[44] C. Kiesling,[32] D. Y. Kim,[54] H. J. Kim,[27] J. B. Kim,[25] J. H. Kim,[24] M. J. Kim,[27] Y. J. Kim,[24] J. Klucar,[21] B. R. Ko,[25] P. Kodyš,[4] S. Korpar,[31,21] P. Krokovny,[3] T. Kuhr,[23] A. Kuzmin,[3] Y.-J. Kwon,[70] S.-H. Lee,[25] J. Li,[53] Y. Li,[67] L. Li Gioi,[32] J. Libby,[15] Y. Liu,[5] D. Liventsev,[11] D. Matvienko,[3] K. Miyabayashi,[38] H. Miyata,[44] R. Mizuk,[20,34] A. Moll,[32,58] N. Muramatsu,[51] R. Mussa,[19] Y. Nagasaka,[12] E. Nakano,[46] M. Nakao,[11] H. Nakazawa,[39] M. Nayak,[15] E. Nedelkovska,[32] C. Ng,[62] M. Niiyama,[26] N. K. Nisar,[57] S. Nishida,[11] O. Nitoh,[65] S. Ogawa,[59] S. Okuno,[22] P. Pakhlov,[20,34] G. Pakhlova,[20] C. W. Park,[55] H. Park,[27] H. K. Park,[27] T. K. Pedlar,[30] T. Peng,[52] R. Pestotnik,[21] M. Petrič,[21] L. E. Piilonen,[67] M. Ritter,[32] M. Röhrken,[23] A. Rostomyan,[6] H. Sahoo,[10] T. Saito,[61] Y. Sakai,[11] S. Sandilya,[57] L. Santelj,[21] T. Sanuki,[61] V. Savinov,[50] O. Schneider,[28] G. Schnell,[1,13] C. Schwanda,[17] D. Semmler,[7] K. Senyo,[69] O. Seon,[36] M. Shapkin,[18] C. P. Shen,[2] T.-A. Shibata,[63] J.-G. Shiu,[41] B. Shwartz,[3] A. Sibidanov,[56] Y.-S. Sohn,[70] A. Sokolov,[18] E. Solovieva,[20] S. Stanič,[45] M. Starič,[21] M. Steder,[6] M. Sumihama,[8] T. Sumiyoshi,[64] U. Tamponi,[19,66] K. Tanida,[53] G. Tatishvili,[47] Y. Teramoto,[46] M. Uchida,[63] S. Uehara,[11] T. Uglov,[20,35] Y. Unno,[9] S. Uno,[11] C. Van Hulse,[1] P. Vanhoefer,[32] G. Varner,[10] A. Vinokurova,[3] V. Vorobyev,[3] M. N. Wagner,[7] C. H. Wang,[40] M.-Z. Wang,[41] P. Wang,[16] M. Watanabe,[44] Y. Watanabe,[22] K. M. Williams,[67] E. Won,[25] Y. Yamashita,[43] S. Yashchenko,[6] Z. P. Zhang,[52] V. Zhilich,[3] V. Zhulanov,[3] and A. Zupanc[23]

(Belle Collaboration)

[1]*University of the Basque Country UPV/EHU, 48080 Bilbao*
[2]*Beihang University, Beijing 100191*
[3]*Budker Institute of Nuclear Physics SB RAS and Novosibirsk State University, Novosibirsk 630090*
[4]*Faculty of Mathematics and Physics, Charles University, 121 16 Prague*
[5]*University of Cincinnati, Cincinnati, Ohio 45221*
[6]*Deutsches Elektronen–Synchrotron, 22607 Hamburg*
[7]*Justus-Liebig-Universität Gießen, 35392 Gießen*
[8]*Gifu University, Gifu 501-1193*
[9]*Hanyang University, Seoul 133-791*
[10]*University of Hawaii, Honolulu, Hawaii 96822*
[11]*High Energy Accelerator Research Organization (KEK), Tsukuba 305-0801*
[12]*Hiroshima Institute of Technology, Hiroshima 731-5193*
[13]*IKERBASQUE, Basque Foundation for Science, 48011 Bilbao*
[14]*Indian Institute of Technology Guwahati, Assam 781039*
[15]*Indian Institute of Technology Madras, Chennai 600036*
[16]*Institute of High Energy Physics, Chinese Academy of Sciences, Beijing 100049*
[17]*Institute of High Energy Physics, Vienna 1050*
[18]*Institute for High Energy Physics, Protvino 142281*
[19]*INFN - Sezione di Torino, 10125 Torino*
[20]*Institute for Theoretical and Experimental Physics, Moscow 117218*
[21]*J. Stefan Institute, 1000 Ljubljana*
[22]*Kanagawa University, Yokohama 221-8686*
[23]*Institut für Experimentelle Kernphysik, Karlsruher Institut für Technologie, 76131 Karlsruhe*
[24]*Korea Institute of Science and Technology Information, Daejeon 305-806*
[25]*Korea University, Seoul 136-713*
[26]*Kyoto University, Kyoto 606-8502*
[27]*Kyungpook National University, Daegu 702-701*
[28]*École Polytechnique Fédérale de Lausanne (EPFL), Lausanne 1015*
[29]*Faculty of Mathematics and Physics, University of Ljubljana, 1000 Ljubljana*
[30]*Luther College, Decorah, Iowa 52101*
[31]*University of Maribor, 2000 Maribor*
[32]*Max-Planck-Institut für Physik, 80805 München*

[33]*School of Physics, University of Melbourne, Victoria 3010*
[34]*Moscow Physical Engineering Institute, Moscow 115409*
[35]*Moscow Institute of Physics and Technology, Moscow Region 141700*
[36]*Graduate School of Science, Nagoya University, Nagoya 464-8602*
[37]*Kobayashi-Maskawa Institute, Nagoya University, Nagoya 464-8602*
[38]*Nara Women's University, Nara 630-8506*
[39]*National Central University, Chung-li 32054*
[40]*National United University, Miao Li 36003*
[41]*Department of Physics, National Taiwan University, Taipei 10617*
[42]*H. Niewodniczanski Institute of Nuclear Physics, Krakow 31-342*
[43]*Nippon Dental University, Niigata 951-8580*
[44]*Niigata University, Niigata 950-2181*
[45]*University of Nova Gorica, 5000 Nova Gorica*
[46]*Osaka City University, Osaka 558-8585*
[47]*Pacific Northwest National Laboratory, Richland, Washington 99352*
[48]*Panjab University, Chandigarh 160014*
[49]*Peking University, Beijing 100871*
[50]*University of Pittsburgh, Pittsburgh, Pennsylvania 15260*
[51]*Research Center for Electron Photon Science, Tohoku University, Sendai 980-8578*
[52]*University of Science and Technology of China, Hefei 230026*
[53]*Seoul National University, Seoul 151-742*
[54]*Soongsil University, Seoul 156-743*
[55]*Sungkyunkwan University, Suwon 440-746*
[56]*School of Physics, University of Sydney, NSW 2006*
[57]*Tata Institute of Fundamental Research, Mumbai 400005*
[58]*Excellence Cluster Universe, Technische Universität München, 85748 Garching*
[59]*Toho University, Funabashi 274-8510*
[60]*Tohoku Gakuin University, Tagajo 985-8537*
[61]*Tohoku University, Sendai 980-8578*
[62]*Department of Physics, University of Tokyo, Tokyo 113-0033*
[63]*Tokyo Institute of Technology, Tokyo 152-8550*
[64]*Tokyo Metropolitan University, Tokyo 192-0397*
[65]*Tokyo University of Agriculture and Technology, Tokyo 184-8588*
[66]*University of Torino, 10124 Torino*
[67]*CNP, Virginia Polytechnic Institute and State University, Blacksburg, Virginia 24061*
[68]*Wayne State University, Detroit, Michigan 48202*
[69]*Yamagata University, Yamagata 990-8560*
[70]*Yonsei University, Seoul 120-749*

(Received 3 December 2013; published 17 March 2014)

We report results of a study of doubly charmed baryons and charmed strange baryons. The analysis is performed using a 980 fb^{-1} data sample collected with the Belle detector at the KEKB asymmetric-energy e^+e^- collider. We search for doubly charmed baryons $\Xi_{cc}^{+(+)}$ with the $\Lambda_c^+ K^-\pi^+(\pi^+)$ and $\Xi_c^0\pi^+(\pi^+)$ final states. No significant signal is observed. We also search for two excited charmed strange baryons, $\Xi_c(3055)^+$ and $\Xi_c(3123)^+$ with the $\Sigma_c^{++}(2455)K^-$ and $\Sigma_c^{++}(2520)K^-$ final states. The $\Xi_c(3055)^+$ signal is observed with a significance of 6.6 standard deviations including systematic uncertainty, while no signature of the $\Xi_c(3123)^+$ is seen. We also study properties of the $\Xi_c(2645)^+$ and measure a width of $2.6 \pm 0.2(\text{stat}) \pm 0.4(\text{syst})$ MeV/c^2, which is the first significant determination.

DOI: 10.1103/PhysRevD.89.052003 PACS numbers: 14.20.Lq, 14.20.-c, 14.20.Gk

I. INTRODUCTION

In recent years, there has been significant progress in charmed baryon spectroscopy, mainly by the Belle and *BABAR* experiments [1–8]. In particular, all the ground states of the single-charmed baryons predicted by the constituent quark model and several excited states have been observed [9].

However, there are no experimentally established doubly charmed baryons. The lightest doubly charmed baryon contains two charm quarks and one up or down quark ($\Xi_{cc}^+ = ccd$, $\Xi_{cc}^{++} = ccu$), and the spin-parity of the ground state is expected to be $\frac{1}{2}^+$. The mass of the Ξ_{cc} has been extensively studied theoretically, and the prediction of the quark model ranges from 3.48 GeV/c^2 to 3.74 GeV/c^2

[10–22], whereas the mass predicted by lattice QCD ranges from 3.51 GeV/c^2 to 3.67 GeV/c^2 [23–27]. The cross sections of the Ξ_{cc} production in the process $e^+e^- \to \Xi_{cc}X$ at $\sqrt{s} = 10.58$ GeV, where X denotes the remaining particles produced in the fragmentation, is predicted to be 70 fb in Ref. [28] and 230 fb in Ref. [29]. The cross section of the pair production of the cc and $\bar{c}\,\bar{c}$ diquarks is predicted to be 7 fb [30].

There have been several experimental studies to search for the Ξ_{cc}. The SELEX collaboration reported evidence for the Ξ_{cc}^+ in the $\Lambda_c^+K^-\pi^+$ [31] and pD^+K^- [32] final states with a mass of about 3.52 GeV/c^2 using a 600 GeV/c charged hyperon beam. However, the results have not been supported by FOCUS [33], *BABAR* [34], Belle [2] nor LHCb [35]. The *BABAR* collaboration searched for the $\Xi_{cc}^{+(+)}$ in the $\Lambda_c^+K^-\pi^+(\pi^+)$ and $\Xi_c^0\pi^+(\pi^+)$ decay modes with a 232 fb^{-1} data sample of e^+e^- collisions at or near the $\Upsilon(4S)$. They found no evidence for the $\Xi_{cc}^{+(+)}$ and set an upper limit on the product of the production cross section and branching fractions of Ξ_{cc} and Λ_c^+ or Ξ_c^0 to be a few fb, depending on the decay mode. In our search for the Ξ_{cc}^+ in the $\Lambda_c^+K^-\pi^+$ final state with a 462 fb^{-1} data sample of Belle at or near the $\Upsilon(4S)$ [2], Belle also found no evidence for the Ξ_{cc}^+ and set an upper limit on $\sigma(e^+e^- \to \Xi_{cc}^+X) \times \mathcal{B}(\Xi_{cc}^+ \to \Lambda_c^+K^-\pi^+)/\sigma(e^+e^- \to \Lambda_c^+X)$ of 1.5×10^{-4} with a $p^*(\Lambda_c^+) > 2.5$ GeV/c requirement. Here, $p^*(\Lambda_c^+)$ is the momentum of the Λ_c^+ in the center-of-mass (CM) frame.

In this paper, we report on an improved search for the Ξ_{cc} in its weak decays to the $\Lambda_c^+K^-\pi^+(\pi^+)$ and $\Xi_c^0\pi^+(\pi^+)$ final states. The Belle collaboration has collected a data sample with a total integrated luminosity of 980 fb^{-1}, which is around two (four) times the statistics of the previous Ξ_{cc} search by Belle [2] (*BABAR* [34]) and supersedes the results in Ref. [2]. Furthermore, in the previous studies, the Λ_c^+ and the Ξ_c^0 states have been reconstructed only from decay modes of $pK^-\pi^+$ and $\Xi^-\pi^+$, respectively. We incorporate additional decay modes to improve the statistical sensitivity.

The same data sample can be used to study charmed strange baryons, as the $\Lambda_c^+K^-\pi^+$ and the $\Xi_c^0\pi^+$ final states are strong decay modes of excited Ξ_c^+ (Ξ_c^{*+}) states. The *BABAR* collaboration found two Ξ_c^{*+} states, $\Xi_c(3055)^+$ and $\Xi_c(3123)^+$, decaying to the $\Lambda_c^+K^-\pi^+$ final state through intermediate $\Sigma_c(2455)^{++}$ or $\Sigma_c(2520)^{++}$ states using a data sample of 384 fb^{-1} [6]. Their statistical significance was 6.4 standard deviations (σ) and 3.6σ, respectively. A confirmation of these states in other experiments is necessary. The $\Xi_c^0\pi^+$ is a strong decay mode of the $\Xi_c(2645)^+$. Currently, only the upper limit of 3.1 MeV/c^2 exists for its width [36]. In this paper, we also report on a search for the $\Xi_c(3055)^+$ and $\Xi_c(3123)^+$ in the $\Lambda_c^+K^-\pi^+$ final state, and the measurement of the width of the $\Xi_c(2645)^+$.

The remaining sections of the paper are organized as follows. In Sec. II, the data samples and the Belle detector are described. In Sec. III, a study of the final states with Λ_c^+, i.e., the Ξ_{cc} search and the $\Xi_c(3055)^+$ and $\Xi_c(3123)^+$ search, are reported. In Sec. IV, a study of the final state with Ξ_c^0 i.e., the Ξ_{cc} search and measurement of the width of the $\Xi_c(2645)^+$, are described. Finally, conclusions are given in Sec. V.

II. DATA SAMPLES AND THE BELLE DETECTOR

We use a data sample with a total integrated luminosity of 980 fb^{-1} recorded with the Belle detector at the KEKB asymmetric-energy e^+e^- collider [37]. The data samples with different beam energies at or near the $\Upsilon(1S)$ to $\Upsilon(5S)$ are combined in this study. The beam energies and integrated luminosities are summarized in Table I. The luminosity-weighted average of $\sqrt{s}$ is 10.59 GeV.

The Belle detector is a large-solid-angle magnetic spectrometer that consists of a silicon vertex detector (SVD), a 50-layer central drift chamber (CDC), an array of aerogel threshold Cherenkov counters (ACC), a barrel-like arrangement of time-of-flight scintillation counters (TOF), and an electromagnetic calorimeter comprised of CsI(Tl) crystals (ECL) located inside a superconducting solenoid coil that provides a 1.5 T magnetic field. An iron flux return located outside of the coil is instrumented to detect K_L^0 mesons and to identify muons (KLM). The detector is described in detail elsewhere [38]. Two inner detector configurations were used. A 2.0 cm radius beampipe and a 3-layer silicon vertex detector were used for the first sample of 156 fb^{-1}, while a 1.5 cm radius beampipe, a 4-layer silicon detector and a small-cell inner drift chamber were used to record the remaining 824 fb^{-1} [39].

The selection of charged hadrons is based on information from the tracking system (SVD and CDC) and hadron identification system (CDC, ACC, and TOF). The charged proton, kaon, and pion that are not associated with long-lived particles like K_S^0, Λ and Ξ^-, are required to have a point of closest approach to the interaction point that is within 0.2 cm in the transverse (r-ϕ) direction and within 2 cm along the z-axis. (The z-axis is opposite the positron beam direction.) For each track, the likelihood values $\mathcal{L}_p$,

TABLE I. Summary of the integrated luminosities and beam energies.

$\sqrt{s}$	$\Upsilon(5S)$/near it	$\Upsilon(4S)$/near it	$\Upsilon(3S)$/near it	$\Upsilon(2S)$/near it	$\Upsilon(1S)$/near it
Integrated luminosity (fb^{-1})	121.0/29.3	702.6/89.5	2.9/0.3	24.9/1.8	5.7/1.8

$\mathcal{L}_K$, and $\mathcal{L}_\pi$ are provided for the assumption of proton, kaon, and pion, respectively, from the hadron identification system, based on the ionization energy loss in the CDC, the number of detected Cherenkov photons in the ACC, and the time of flight measured by the TOF. The likelihood ratio is defined as $\mathcal{L}(i:j) = \mathcal{L}_i/(\mathcal{L}_i + \mathcal{L}_j)$ and a track is identified as a proton if the likelihood ratios $\mathcal{L}(p:\pi)$ and $\mathcal{L}(p:K)$ are greater than 0.6. A track is identified as a kaon if the likelihood ratios $\mathcal{L}(K:\pi)$ and $\mathcal{L}(K:p)$ are greater than 0.6. A track is identified as a pion if the likelihood ratios $\mathcal{L}(\pi:K)$ and $\mathcal{L}(\pi:p)$ are greater than 0.6. In addition, electron ($\mathcal{L}_e$) likelihood is provided based on information from the ECL, ACC, and CDC [40]. A track with an electron likelihood greater than 0.95 is rejected.

The momentum averaged efficiencies of hadron identification are about 90%, 90%, and 93% for pions, kaons, and protons, respectively. The momentum averaged probability to misidentify a pion (kaon) track as a kaon (pion) track is about 9 (10)%, and the momentum averaged probability to misidentify a pion or kaon track as a proton track is about 5%.

We use a Monte-Carlo (MC) simulation events generated with EVTGEN [41], JETSET [42] with final QED final state radiation by PHOTOS [43] and then processed by a GEANT3 [44] based detector simulation to obtain the reconstruction efficiency and the mass resolution.

III. FINAL STATE WITH THE Λ_c^+

In this section, the analysis using the final states with the Λ_c^+ baryon is described. Reconstruction of the Λ_c^+ candidate is explained first, followed by the description of the $\Xi_{cc}^{+(+)}$ search in its decay into $\Lambda_c^+ K^- \pi^+ (\pi^+)$ and the study of two charmed strange baryons, $\Xi_c(3055)^+$ and $\Xi_c(3123)^+$. Throughout this paper, the selection criteria are determined to maximize the figure of merit (FOM), defined as $\varepsilon/\sqrt{N_{\rm bg}}$, where ε is the Ξ_{cc} efficiency for the selection criteria and $N_{\rm bg}$ is the number of background events under the signal peak except for the scaled momentum selection for the $\Xi_c(3055)^+$ and $\Xi_c(3123)^+$ search, which followed *BABAR*'s analysis. The distribution of background events is estimated based on data. When the selection criteria are determined, we hide the possible signal peak by smearing the invariant mass of the Ξ_{cc} candidates event by event with a Gaussian having a 50 MeV/c^2 width in order to avoid any biases.

A. Reconstruction of the Λ_c^+

The Λ_c^+ candidates are reconstructed in the $pK^-\pi^+$ and pK_S^0 decay modes [45]. The K_S^0 candidate is reconstructed from its decay into $\pi^+\pi^-$. A pair of oppositely charged pions that have an invariant mass within 8 MeV/c^2 of the nominal K_S^0 mass, which corresponds to approximately 3.5σ of the mass resolution, is used. Two pion tracks are fitted to a common vertex. The result of the fit is used to suppress misreconstructed K_S^0 candidates and to perform further vertex fit of the $\Lambda_c^+ \to pK_S^0$. The vertex of the two pions for the K_S^0 is required to be displaced from the interaction point (IP) in the direction of the pion pair momentum [46]. The daughters of the Λ_c^+ are fitted to a common vertex; the invariant mass of the daughters must be within 5(6) MeV/c^2, or 1.5σ, nominal Λ_c^+ mass for the $pK^-\pi^+$ (pK_S^0) decay mode. The χ^2 value of the common vertex fit of the Λ_c^+ is required to be less than 50. For the remaining candidate, a mass constraint fit to the Λ_c^+ mass is performed to improve the momentum resolution. As the signal-to-background ratio for the Λ_c^+ candidates is similar for the $pK^-\pi^+$ and pK_S^0 decay modes, they are combined in the following analysis. By including the pK_S^0 mode in addition to the $pK^-\pi^+$ mode, the yield of the Λ_c^+ is increased by about 20%.

B. Search for doubly charmed baryons in $\Lambda_c^+ K^- \pi^+ (\pi^+)$

We search for the $\Xi_{cc}^{+(+)}$ in its decay into $\Lambda_c^+ K^- \pi^+ (\pi^+)$ in the mass range of 3.2–4.0 GeV/c^2. The expected mass resolution of the Ξ_{cc} estimated from MC is 2.0–3.5 MeV/c^2, depending on the mass of the Ξ_{cc} (degrading with increasing mass). In order to reduce the combinatorial background, a selection on the scaled momentum $x_p = p^*\sqrt{s/4 - m^2}$ is used, where p^* is the CM momentum of a Ξ_{cc} candidate and s is CM energy squared and m is mass of the Ξ_{cc} candidate. As there is no measurement of the x_p spectrum for Ξ_{cc} production, we assume it to be the same as that of the Λ_c^+, which has been precisely measured [47]. The x_p spectrum is represented by a smooth polynomial function and is used to generate a MC sample for the Ξ_{cc} signal. Decays of the Ξ_{cc} and Λ_c^+ are generated according to the available phase space distribution. The number of background events as a function of the x_p cut is estimated based on smeared data. The FOM as a function of the x_p cut is surveyed in the search region. The optimization procedure yields $0.5 < x_p < 1.0$ regardless of the Ξ_{cc} mass. To check the validity of our analysis, we independently examine the x_p spectrum of the Λ_c^+ and confirm that it is consistent with that presented in Ref. [47].

Figure 1(a) and 1(b) show the $M(\Lambda_c^+ K^- \pi^+)$ and $M(\Lambda_c^+ K^- \pi^+ \pi^+)$ distributions, respectively, for data after all the event selections are applied. No significant signal is seen in the data for either Ξ_{cc}^+ or Ξ_{cc}^{++}. The statistical significance for a given mass is evaluated with an unbinned extended maximum likelihood (UML) fit. The probability density function (PDF) for the signal is described with signal MC generated for each given Ξ_{cc} mass, whereas a third-order polynomial function is used as the background PDF. The statistical significance is defined as $\sqrt{-2\ln(\mathcal{L}_0/\mathcal{L})}$, where $\mathcal{L}_0$ is the likelihood for the fit without the signal component and $\mathcal{L}$ is the likelihood for the fit with the signal component included. The significance is evaluated for the Ξ_{cc} mass

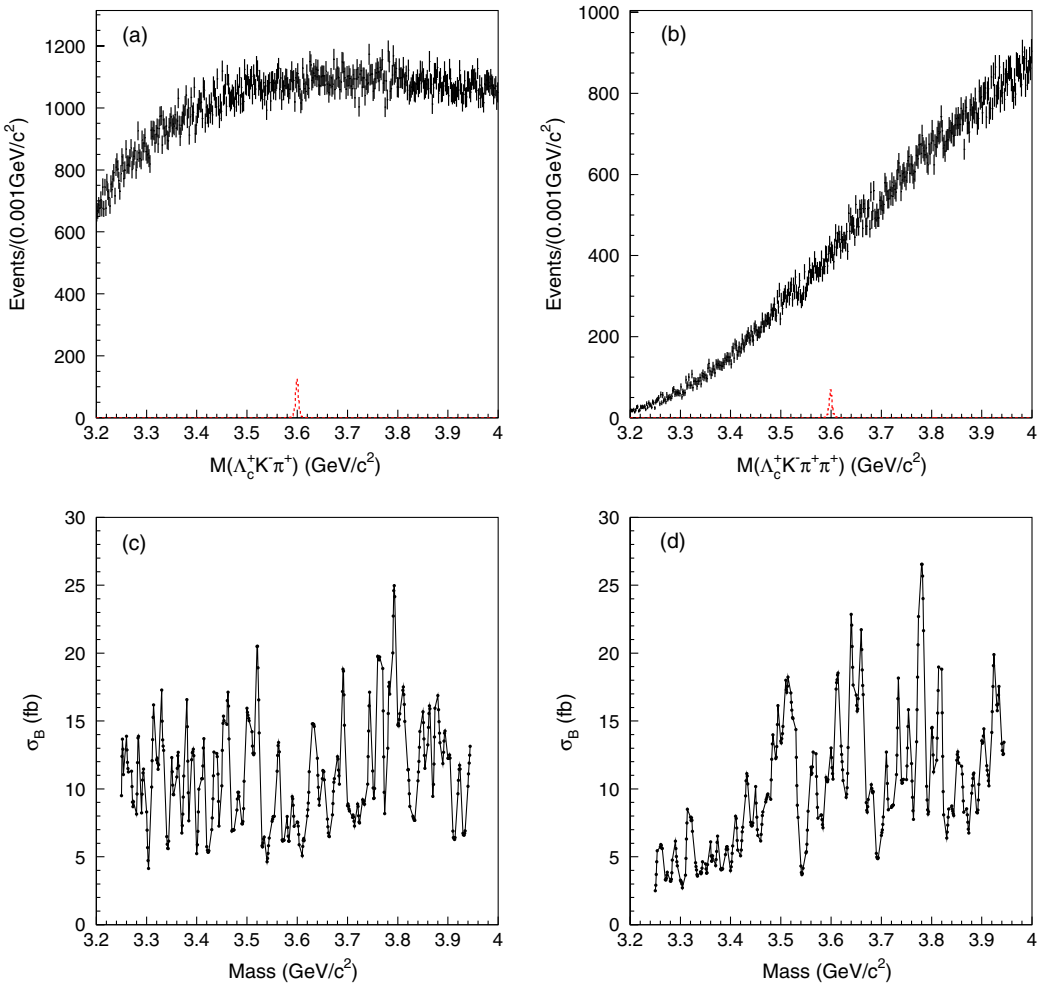

FIG. 1 (color online). Invariant mass distribution of the Ξ_{cc} candidates for (a) $M(\Lambda_c^+ K^- \pi^+)$, (b) $M(\Lambda_c^+ K^- \pi^+ \pi^+)$; the vertical error bars are from data and the dashed histogram are from signal MC for the Ξ_{cc} signal generated with a mass of 3.60 GeV/c^2 and a production cross section $\sigma(e^+e^- \to \Xi_{cc}^{+(+)} X)$ of 500 fb and $\mathcal{B}(\Xi_{cc}^{+(+)} \to \Lambda_c^+ K^- \pi^+(\pi^+))$ of 5%. 95% C.L. upper limit of $\sigma_{\mathcal{B}}$ as a function of the mass with a 1 MeV/c^2 step for (c) Ξ_{cc}^+ and (d) Ξ_{cc}^{++}.

scanned with a 1 MeV/c^2 step in the search region. None of the mass points give a significance exceeding the 3σ level.

The 95% confidence level (C.L.) upper limit for the product of the cross section and branching fraction to the $\Lambda_c K^- \pi^+(\pi^+)$ state produced with the $0.5 < x_p < 1.0$ condition,

$$\sigma_{\mathcal{B}} \equiv \sigma(e^+e^- \to \Xi_{cc}^{+(+)} X)$$

is evaluated. Here, L is the total integrated luminosity, $N_{\rm sig}$ is the Ξ_{cc} signal yield, $\mathcal{B}_{pK^-\pi^+}$ is the branching fraction of the $\Lambda_c^+ \to pK^-\pi^+$ (which amounts to 0.050 ± 0.013), $\mathcal{B}_{pK_S}$ is the branching fraction of $\Lambda_c^+ \to pK_S^0$ measured relative to the $pK^-\pi^+$ mode ($\mathcal{B}_{pK_S}/\mathcal{B}_{pK^-\pi^+} = 0.24 \pm 0.02$), and $\varepsilon_{pK^-\pi^+(pK_S)}$ is the reconstruction efficiency for the $\Lambda_c^+ \to pK^-\pi^+$ ($\Lambda_c^+ \to pK_S^0$) decay mode evaluated as a function of the Ξ_{cc} mass. The efficiencies for the $\Xi_{cc}^{+(+)}$ as a function of their masses are shown in Fig. 2. The factor of two in the denominator comes from inclusion of the charge-conjugate mode. By including this factor, our measurement can be compared with the theoretical predictions [28,29]; while to compare with the prediction in Ref. [30], it is necessary to multiply our $\sigma_{\mathcal{B}}$ measurement by 2 because they predicted the cross section of the pair production of the cc and $\bar{c}\,\bar{c}$ diquarks. In *BABAR*'s measurement [34], they do not introduce the factor of two, i.e., they report an upper limit for the sum of the $\sigma(e^+e^- \to \Xi_{cc}^{+(+)} X)$ and its charge-conjugate mode). Therefore, our measurement should be doubled when comparing with *BABAR*'s result. We note that the cross section reported here and elsewhere in this paper is a visible cross section (i.e., a radiative correction is not applied.

The upper limit is evaluated following the Bayesian approach. First, we scan the likelihood profile by determining the likelihood values as a function of the $\sigma_{\mathcal{B}}$ ($\mathcal{L}(\sigma_{\mathcal{B}})$),

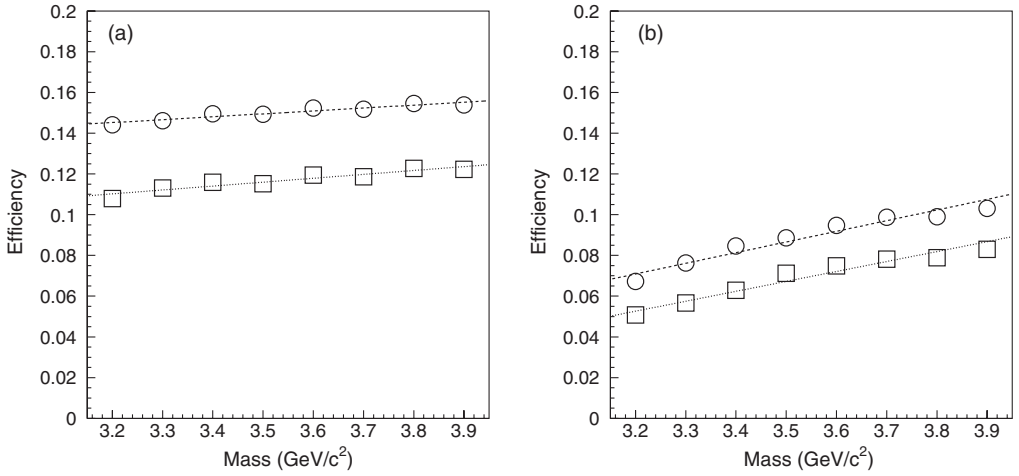

FIG. 2. Reconstruction efficiency as a function of the Ξ_{cc} mass, for (a) Ξ_{cc}^{+}, (b) Ξ_{cc}^{++}. Circular points are for $\Lambda_c^+ \to pK^-\pi^+$ and square points are for $\Lambda_c^+ \to pK_S^0$. The lines show the result of the fit with a linear function.

varying $N_{\rm sig}$ from zero up to the $N_{\rm sig}$ value for which the likelihood drops to zero. Then, $\mathcal{L}(\sigma_{\mathcal{B}})$ is convolved with a Gaussian whose width equals the systematic uncertainties of $\sigma_{\mathcal{B}}$. The $\sigma_{\mathcal{B}}$ value for which the integral (starting from $\sigma_{\mathcal{B}} = 0$) becomes 95% of the entire area is regarded as the 95% C.L. upper limit.

We consider the following systematic uncertainties in the Ξ_{cc} search. The systematic uncertainty due to the efficiency of pion and kaon identification is estimated from the ratio of the yield of the $D^{*+} \to D^0\pi^+$, $D^0 \to K^-\pi^+$ with and without the pion/kaon identification requirements for data and MC. The difference of the ratio between data and MC is corrected and the statistical error of the ratio is regarded as the systematic uncertainty. The systematic uncertainty due to the efficiency of proton identification is estimated using the ratio of the yield of the $\Lambda \to p\pi^-$ with and without the proton identification requirement. The difference of the ratio between data and MC is corrected and the statistical error of the ratio is regarded as the systematic uncertainty. The systematic uncertainty due to the charged track reconstruction efficiency is estimated using the decay chain $D^{*+} \to \pi^+ D^0$, $D^0 \to \pi^+\pi^- K_S^0$, and $K_S^0 \to \pi^+\pi^-$, where $K_S^0 \to \pi^+\pi^-$ is either partially or fully reconstructed. The ratio of the yields for partially and fully reconstructed signals in data and MC is compared, and the difference is taken as the systematic uncertainty. This amounts to 0.35% per track. The systematic uncertainty of the total integrated luminosity is 1.4%. To check the systematic error due to the signal PDF, we compare the mass resolution of the Λ_c^+ in data and MC. We find that the resolution for data is 5% larger than in MC. To monitor the effect of this discrepancy, we perform a pseudoexperiment test in which we extract the signal yield with correct PDF and one that is narrower by 5%. The largest difference of 3% measured in this test is regarded as the systematic uncertainty. The systematic uncertainty related to the Λ_c^+ branching fraction is propagated from the errors taken from the PDG [9]. To estimate the systematic uncertainty of the reconstruction efficiency due to the possible difference of x_p spectrum between our assumption (the same as that of Λ_c^+) and the actual one, we examine the x_p dependence of the reconstruction efficiency. The root mean square of the reconstruction efficiency in the region of $0.5 < x_p < 1.0$ is regarded as the systematic uncertainty. The elements of the systematic uncertainty for the measurement of the $\sigma_{\mathcal{B}}$ are enumerated in the first and second columns of Table II.

Figures 1(c) and 1(d) show the 95% C.L. upper limit on $\sigma_{\mathcal{B}}$ for Ξ_{cc}^{+} and Ξ_{cc}^{++}, respectively, as a function of the mass

TABLE II. Summary of the systematic uncertainties in the $\sigma_{\mathcal{B}}$ and $\sigma_{\mathcal{B}^2}$ measurement (%).

Source	Ξ_{cc}^{+} with Λ_c^+	Ξ_{cc}^{++} with Λ_c^+	$\Xi_c(3123)^+$	Ξ_{cc}^{+} with Ξ_c^0	Ξ_{cc}^{++} with Ξ_c^0
Particle ID	2.0	2.4	2.0	3.5	3.8
Tracking	1.8	2.1	1.8	1.8	2.1
Signal PDF	3.5	3.5	28.0	3.5	3.5
Luminosity	1.4	1.4	1.4	1.4	1.4
$\mathcal{B}$	26.0	26.0	1.6	0.7	0.7
x_p	2.1	2.3	1.2	6.0	5.7
$N^i_{\Xi_c(2645)^+}$	…	…	…	4.3	4.3
total	26.5	26.6	28.2	9.2	9.2

with a 1 MeV/c^2 step. The upper limit is in the range of 4.1–25.0 fb for the Ξ_{cc}^{+} and 2.5–26.5 fb for the Ξ_{cc}^{++}.

C. Search for the $\Xi_c^+(3055)$ and $\Xi_c^+(3123)$

In this section, a search for the $\Xi_c^+(3055)$ and $\Xi_c^+(3123)$ is described. Here, we require x_p to be greater than 0.7. In the analysis by *BABAR* [6], they required $p^*(\Lambda_c^+K^-\pi^+) > 2.9$ GeV/c, which is similar to our x_p cut as illustrated by the $p^*(\Lambda_c^+K^-\pi^+)$ distribution, with the x_p cut and 2.9 GeV/$c^2 < M(\Lambda_c^+K^-\pi^+) < 3.2$ GeV/c^2 required as shown in Fig. 3(a). Figure 3(b) shows the $M(\Lambda_c^+\pi^+)$ distribution, where contributions from the $\Sigma_c(2455)^{++}$ and the $\Sigma_c(2520)^{++}$ baryons are clearly visible. We select the $\Sigma_c(2455)^{++}$ [$\Sigma_c(2520)^{++}$] region by requiring $|M(\Lambda_c^+\pi^+) - m_{\Sigma_c^{++}}| < 5(18)$ MeV/c^2, where $m_{\Sigma_c^{++}}$ is the nominal mass of the $\Sigma_c(2455)^{++}$ or $\Sigma_c(2520)^{++}$.

Figure 3(c) shows the $M(\Lambda_c^+K^-\pi^+)$ distribution for the $\Sigma_c(2455)^{++}$ signal region together with the same plot for the $\Sigma_c(2455)^{++}$ sideband region, defined as $|M(\Lambda_c^+\pi^+) - (m_{\Sigma_c(2455)^{++}} \pm 15\ \text{MeV}/c^2)| < 5$ MeV/c^2. Clear peaks corresponding to the $\Xi_c(2980)^+$, $\Xi_c(3055)^+$, and $\Xi_c(3080)^+$ are seen. To obtain the statistical significance of the $\Xi_c(3055)^+$, an UML fit is applied. PDFs for the Ξ_c^{*+} components are represented by a Breit-Wigner line shape convolved with a Gaussian to account for the invariant-mass resolution (σ_{res}). Using the signal MC events, we estimate σ_{res} to vary from 1.2 to 1.8 MeV/c^2, depending on the masses of the Ξ_c^{*+} states. The width and mean of the Breit-Wigner functions are treated as free

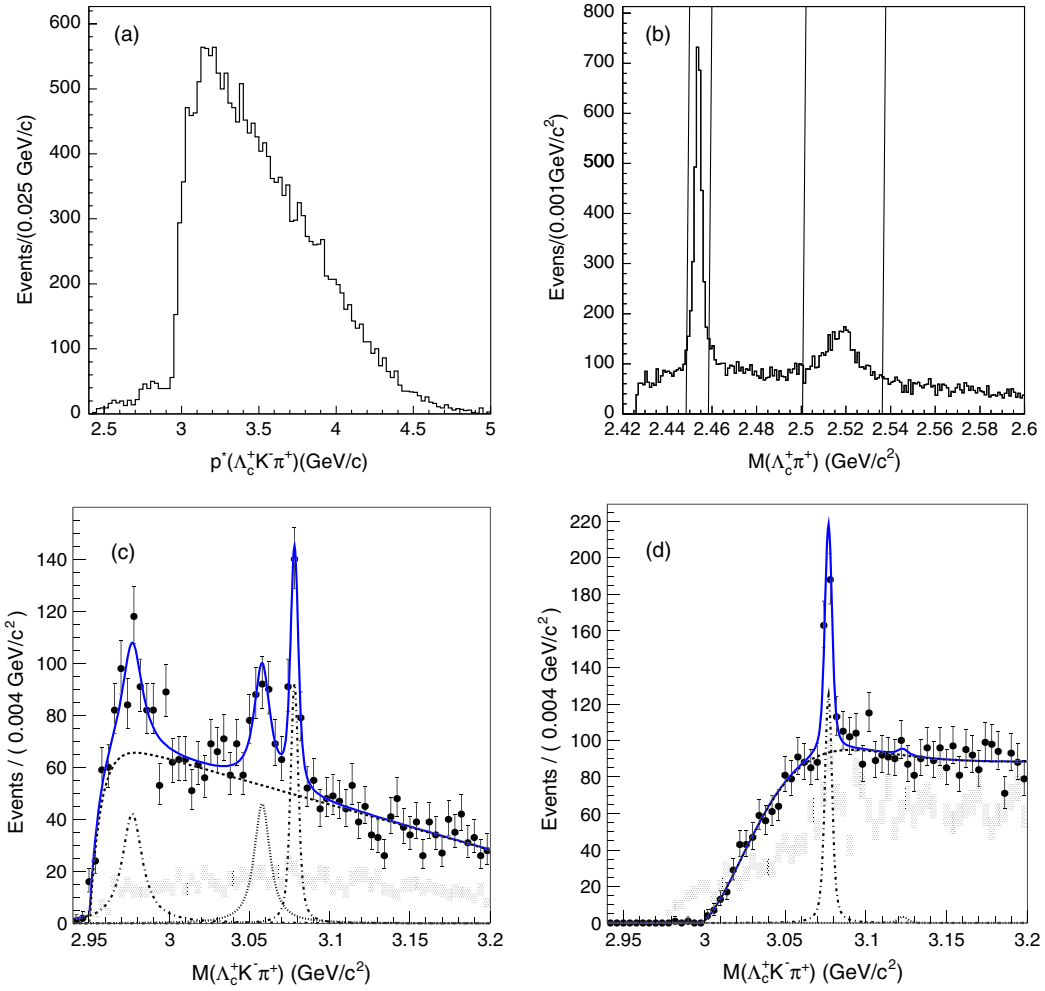

FIG. 3 (color online). (a) The $p^*(\Lambda_c^+K^-\pi^+)$ distribution from data. (b) The $M(\Lambda_c^+\pi^+)$ distribution. The vertical lines show the selected regions of the $\Sigma_c(2455)^{++}$ and $\Sigma_c(2520)^{++}$. (c) The $M(\Lambda_c^+K^-\pi^+)$ distribution with $\Sigma_c(2455)^{++}$ selection. The dots with error bars show the distribution for the $\Sigma_c(2455)^{++}$ selected region whereas the rectangles show the distribution for the $\Sigma_c(2455)^{++}$ sideband region. The solid line shows the fit result. The dashed, dotted, and dash-dotted lines show the contributions from the background, $\Xi_c(3055)^+$, and $\Xi_c(2980)^+$, or $\Xi_c(3080)^+$, respectively. (d) The $M(\Lambda_c^+K^-\pi^+)$ distribution with $\Sigma_c(2520)^{++}$ selection. The dots with error bars show the distribution for $\Sigma_c(2520)^{++}$ selected region whereas the rectangles show the distribution for the $\Sigma_c(2520)^{++}$ sideband region. The solid line shows the fit result. The dashed, dotted, and dash-dotted lines show the contributions from the background, $\Xi_c(3123)^+$, and $\Xi_c(3080)^+$, respectively.

parameters. The background PDF, $f_1(x)$, is modeled with a threshold function:

$$f_1(x) = 1 - \exp((x - x_0)/\delta_m)(x/x_0)^a + b(x/x_0 - 1) \quad (\text{if } x > x_0)$$
$$f_1(x) = 0 \quad (\text{if } x < x_0), \tag{1}$$

where a, b, x_0, and δ_m are free parameters in the fit.

The fit result is shown in Fig. 3(c). To estimate the statistical significance of the $\Xi_c(3055)^+$, we compare the likelihood values for the fits with and without the $\Xi_c(3055)^+$ component. The obtained $-2\ln(\mathcal{L}_0/\mathcal{L})$ value is 54.7. By taking into account the change of the number of degrees of freedom (ndf) by the inclusion of the $\Xi_c(3055)^+$ component, the statistical significance of the $\Xi_c(3055)^+$ becomes 6.8σ. The χ^2/ndf of the fit with the $\Xi_c(3055)^+$ component, for the binning of Fig. 3(c), is 54.8/61.

Figure 3(d) shows the $M(\Lambda_c^+ K^- \pi^+)$ distribution for the $\Sigma_c(2520)^{++}$ selected region together with the same plot for the $\Sigma_c(2520)^{++}$ sideband region, defined as $|M(\Lambda_c^+\pi^+) - (m_{\Sigma_c(2520)^{++}} \pm 27\ \text{MeV}/c^2)| < 12\ \text{MeV}/c^2$. A clear peak corresponding to the $\Xi_c(3080)^+$ is seen, while no peak structure is seen in the mass near 3.123 GeV/c^2. An UML fit is applied to extract the signal yield. Again, the Ξ_c^{*+} components are represented by a Breit-Wigner function convolved with a Gaussian. For the $\Xi_c(3080)^+$ component, the mass and width of the Breit-Wigner are treated as free parameters; while for the $\Xi_c(3123)^+$ component, the mass and width are fixed to the values obtained in Ref.[6]. The background shape, $f_2(x)$, is assumed to be:

$$f_2(x) = (1 - \exp((x - x_0)^2/\delta_m))(x/x_0)^a + b(x/x_0 - 1) + c((x/x_0)^2 - 1) \quad (\text{if } x > x_0)$$
$$f_2(x) = 0 \quad (\text{if } x < x_0), \tag{2}$$

where a, b, c, x_0, and δ_m are fit parameters. The χ^2/ndf of the fit with the $\Xi_c(3123)^+$ component for the binning of Fig. 3(d) is 28.6/42. The yield of the $\Xi_c(3123)^+$ is 8 ± 22 events, which is consistent with zero. Hence, a 95% C.L. upper limit for the production cross section is evaluated with the method described in the previous section. To directly compare with the *BABAR* result in Ref. [6], the upper limit for the product of the cross section and branching fraction of Λ_c^+ produced with $x_p > 0.7$ condition,

$$\sigma_{\mathcal{B}\Lambda_c^+} \equiv \sigma(e^+e^- \to \Xi_c(3123)^+ X) \times \mathcal{B}(\Lambda_c^+ \to pK^-\pi^+)$$

is evaluated. As in Ref. [6], we assume $\mathcal{B}(\Xi_c(3123)^+ \to \Sigma_c(2520)^{++}K^-)$ is equal to 1.

To take the uncertainty of the $\Xi_c(3123)^+$ mass and width from Ref. [6] into account, we perform a pseudoexperiment test. The background and $\Xi_c(3080)^+$ contributions are generated with statistics similar to data and based on the fit result. The $\Xi_c(3123)^+$ component is generated with mass and width changed by $\pm 1\sigma$, corresponding to their measured uncertainties ($3122.9 \pm 1.3 \pm 0.4$ MeV/c^2 for the mass and $4.4 \pm 3.4 \pm 1.7$ MeV/c^2 for the width). The yield of $\Xi_c(3123)^+$ is extracted by fitting pseudoexperiment data with the procedure used for data. The ratio of the generated and extracted yield is regarded as a systematic uncertainty. Because the error of the width is relatively large, its systematic uncertainty contribution is dominant (28%). All of the systematic errors are summarized in the third column of Table II. The 95% C.L. upper limit on $\sigma_{\mathcal{B}\Lambda_c^+}$ is 0.17 fb. As in the case of the Ξ_{cc} cross section, the measurement in Ref. [6] does not introduce a factor of two for the $\sigma_{\mathcal{B}\Lambda_c^+}$ calculation. Therefore, we should double our measurement, which results in 0.34 fb, when comparing with *BABAR*'s result. The value is much smaller than that quoted in Ref. [6] ($1.6 \pm 0.6 \pm 0.2$ fb).

The systematic uncertainties of the masses and widths of the Ξ_c^{*+} and stability of the statistical significance of the $\Xi_c(3055)^+$ are studied by the following fitting configurations. The systematic uncertainties due to the signal PDF are studied by varying σ_{res} by 5%. The systematic uncertainties due to possible interference between the $\Xi_c(3055)^+$ and $\Xi_c(3080)^+$ are studied by fitting the distribution with an additional phase parameter between the two Breit-Wigner amplitudes. The systematic uncertainty due to the background shape is studied by fitting the mass spectra with a second-order polynomial as a background PDF in the range of 3.005–3.200 GeV/c^2. In none of these fitting configurations does the statistical significance of the $\Xi_c(3055)^+$ fall below 6.6σ. We apply cut conditions of $x_p > 0.6$ and $x_p > 0.8$ instead of $x_p > 0.7$ and reextract the masses and widths of the Ξ_c^{*+} states. The differences from the default cut condition are regarded as systematic uncertainties. The measured masses, widths, and yields of the three Ξ_c^{*+} states are summarized in Table III. All of these measurements are consistent with previous Belle measurement [2] within 2.5σ and with the *BABAR* measurement [6] within 2.0σ.

TABLE III. The measured masses and widths of the three Ξ_c^{*+} states. The first error is statistical and second is systematic.

Particle	Mass (MeV/c^2)	Width (MeV/c^2)	Yield
$\Xi_c(2980)^+$	$2974.9 \pm 1.5 \pm 2.1$	$14.8 \pm 2.5 \pm 4.1$	244 ± 39
$\Xi_c(3055)^+$	$3058.1 \pm 1.0 \pm 2.1$	$9.7 \pm 3.4 \pm 3.3$	199 ± 46
$\Xi_c(3080)^+$ (Σ_c)	$3077.9 \pm 0.4 \pm 0.7$	$3.2 \pm 1.3 \pm 1.3$	185 ± 31
$\Xi_c(3080)^+$ (Σ_c^*)	$3076.9 \pm 0.3 \pm 0.2$	$2.4 \pm 0.9 \pm 1.6$	210 ± 30

IV. FINAL STATE WITH Ξ_c^0

In this section, the analysis of the final state with the Ξ_c^0 is described. The reconstruction of the Ξ_c^0 is presented first, followed by the analysis of the $\Xi_c(2645)^+$. Finally, a search for $\Xi_{cc}^{+(+)}$ decaying into the $\Xi_c^0\pi^+(\pi^+)$ final state is described.

A. Reconstruction of Ξ_c^0

The Ξ_c^0 is reconstructed in three decay modes: $\Xi^-\pi^+$, $\Lambda K^-\pi^+$, and $pK^-K^-\pi^+$. The Λ is reconstructed from its decay into $p\pi^-$. The proton and π^- tracks for Λ candidates are fitted to a common vertex. The fitting result is used to suppress misreconstructed Λ candidates and to perform the subsequent vertex fit for the $\Xi^- \to \Lambda\pi^-$ or $\Xi_c^0 \to \Lambda K^-\pi^+$. The invariant mass of the Λ candidate is required to be within 3 MeV$/c^2$ of the nominal Λ mass, which corresponds to approximately 3σ of the mass resolution. The selection based on their decay vertex information is also applied [48]. The Ξ^- is reconstructed from its decay into $\Lambda\pi^-$. The Λ and π^- tracks for Ξ^- candidates are fitted to a common vertex. The fitting result is used to clean up the Ξ^- candidates and in the common vertex fit for the $\Xi_c^0 \to \Xi^-\pi^+$. The closest distance of the Λ and π^- along the z-direction is required to be less than 3 mm. We require $\cos\theta > 0.95$, where θ is the angle between the momentum vector of the Ξ^- and the vector between the IP and the Ξ^- decay vertex. The χ^2 of the common-vertex fit of the $\Lambda\pi^-$ is required to be less than 50. The invariant mass of a Ξ^- candidate is required to be within 4 MeV$/c^2$ of the nominal Ξ^- mass, which corresponds to approximately 3σ of the mass resolution. The daughter particles of the Ξ_c^0 are fitted to a common vertex. The Ξ_c^0 candidates are selected by requiring invariant masses of the daughter particles with common vertex fit to be within 12, 7, and 7 MeV$/c^2$ of the nominal Ξ_c^0 mass for the $\Xi^-\pi^+$, $\Lambda K^-\pi^+$, and $pK^-K^-\pi^+$ decay modes, respectively, which correspond to approximately 1.5σ of the mass resolution. The χ^2 value of the common vertex fit for the Ξ_c^0 is required to be less than 50. The mass constraint fit to the Ξ_c^0 mass is performed.

We optimize the selection criteria for x_p in the $\Xi_c^0\pi^+(\pi^+)$ system with the method described in Sec. III B, again assuming that the x_p spectrum for the Ξ_{cc} is the same as that for the Λ_c^+. We require $0.45 < x_p < 1.0$ independent of the Ξ_{cc} mass and the Ξ_c^0 decay mode. The same cut is applied for the analysis of the $\Xi_c(2645)^+$.

B. Study of the $\Xi_c^+(2645)$

Unlike the Λ_c^+ study, the signal-to-background ratio of the Ξ_c^0 largely depends on the decay modes. Therefore, to improve our sensitivity for the Ξ_{cc}, we perform a simultaneous fit to the mass spectra for the three Ξ_c^0 decays with fixed relative signal ratios. We use the relative yields of the $\Xi_c(2645)^+ \to \Xi_c^0\pi^+$ measured for the Ξ_c^0 decay modes to estimate a relative signal yield of the Ξ_{cc}. The relative signal yields of the Ξ_{cc} ($N^i_{\Xi_{cc}}$) in a given Ξ_c^0 decay channel can be written as

$$N^i_{\Xi_{cc}} = N^i_{\Xi_c(2645)^+} \frac{\epsilon^i_{\Xi_{cc}}}{\epsilon^i_{\Xi_c(2645)^+}}, \tag{3}$$

where $N^i_{\Xi_c(2645)^+}$ is the $\Xi_c(2645)^+$ yield, $\epsilon^i_{\Xi_{cc}}$ is the reconstruction efficiency of the Ξ_{cc}, and $\epsilon^i_{\Xi_c(2645)^+}$ is the reconstruction efficiency of the $\Xi_c(2645)^+$. Both efficiencies include the secondary branching fractions for $\Lambda \to p\pi^-$ of $(63.9 \pm 0.5)\%$ and $\Xi^- \to \Lambda\pi^-$ of $(99.887 \pm 0.035)\%$. The index i denotes the decay mode of the Ξ_c^0.

Figure 4 shows the $M(\Xi_c^0\pi^+)$ distribution for each Ξ_c^0 decay mode below the Ξ_{cc} search region. Clear peaks corresponding to the $\Xi_c(2645)^+$ are seen in all decay modes. The bump structures near 2.68 GeV$/c^2$ originate from the process $\Xi_c(2790)^+ \to \Xi_c'^0\pi^+ \to \Xi_c^0\gamma\pi^+$ with a γ missing in the reconstruction. The simultaneous UML fit is applied to extract the relative yields and the width of the $\Xi_c(2645)^+$. The $\Xi_c(2645)^+$ signal is represented by a

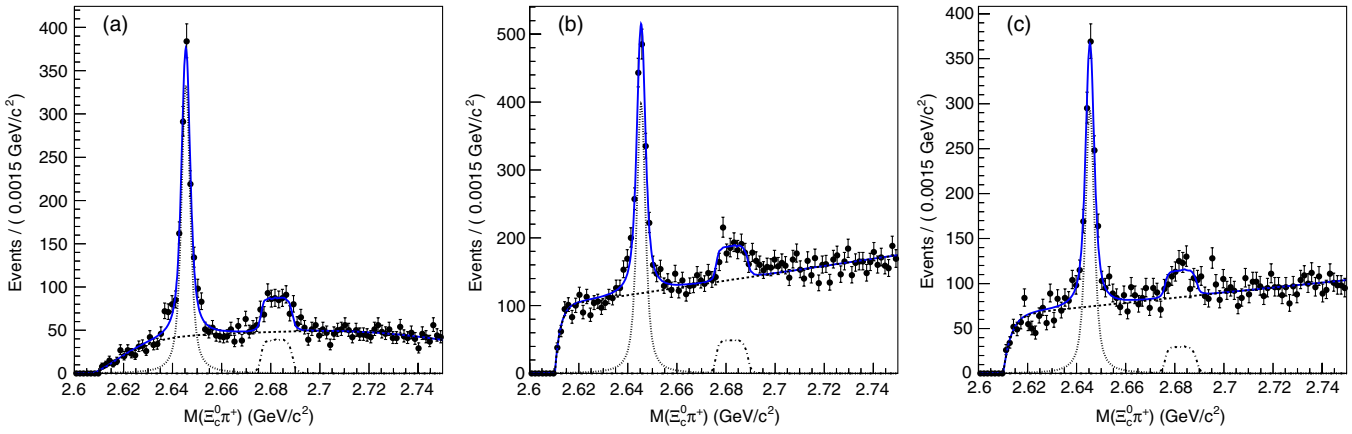

FIG. 4 (color online). $M(\Xi_c^0\pi^+)$ distributions below the Ξ_{cc} search region for (a) $\Xi_c^0 \to \Xi^-\pi^+$, (b) $\Xi_c^0 \to \Lambda K^-\pi^+$, (c) $\Xi_c^0 \to pK^-K^-\pi^+$. The solid lines show the fit result. The dashed, dotted, and dash-dotted lines show the contributions from background, $\Xi_c(2645)^+$, and $\Xi_c(2790)^+$, respectively.

Breit-Wigner function convolved with a Gaussian whose width corresponds to the mass resolution $\sigma_{\rm res}$. The value of $\sigma_{\rm res}$ is 1.05 MeV/c^2, independent of the decay modes of the Ξ_c^0. The PDF of the $\Xi_c(2790)^+$ reflection is modeled using MC. $f_2(x)$ in Eq. (2) is used as the background PDF for the $\Xi_c^0 \to \Xi^-\pi^+$ decay mode whereas $f_1(x)$ in Eq. (1) is used for the $\Xi_c^0 \to \Lambda K^-\pi^+$ and $\Xi_c^0 \to pK^-K^-\pi^+$ decay modes. The width and mass of the $\Xi_c(2645)^+$ are constrained to be the same for the three decay modes. The yield of the $\Xi_c(2645)^+$ is 1298 ± 51, 1444 ± 58, and 974 ± 47 for the $\Xi^-\pi^+$, $\Lambda K^-\pi^+$, and $pK^-K^-\pi^+$ decay mode, respectively. The mass and width are obtained to be 2645.4 ± 0.1 MeV/c^2 and 2.6 ± 0.2 MeV/c^2, respectively. The χ^2/ndf of the fit for the binning in Fig. 4 is 296/276.

To check the consistency of the width measurement between the Ξ_c^0 decay modes, we fit the three mass spectra separately. The measured widths are found to be consistent between the three decay modes: 2.9 ± 0.3 MeV/c^2, 2.6 ± 0.3 MeV/c^2, and 2.5 ± 0.3 MeV/c^2 for $\Xi_c^0 \to \Xi^-\pi^+$, $\Lambda K^-\pi^+$, and $pK^-K^-\pi^+$, respectively. The measured width is found to be consistent for the three decay modes. The systematic uncertainty of the width measurement due to the fit procedure is studied with pseudoexperiment events samples: the $\Xi_c(2645)^+$ component is generated according to the signal MC sample with the natural width of 2.6 MeV/c^2 by signal MC, while contributions from background and $\Xi_c(2790)^+$ reflection are generated based on the fit result with the real data. The statistics of the pseudoexperiment samples are the same as for those of data. The width of the $\Xi_c(2645)^+$ is extracted from simultaneous fits to pseudoexperiment samples, and its mean value is obtained to be 2.75 ± 0.03 MeV/c^2, which is higher than the input value by 0.15 MeV/c^2. The difference is included as the systematic uncertainty from the fit procedure. The systematic uncertainty due to the background shape is studied by fitting the data with a second-order polynomial function for the alternative background shape. The fit region is restricted to 2.62–2.75 GeV/c^2. The width is obtained to be 2.9 ± 0.2 MeV/c^2, which is 0.3 MeV/c^2 higher than the default measurement. This deviation is included as a systematic uncertainty. To check the systematic uncertainty due to the mass resolution, we evaluate the ratio of the resolution of the Ξ_c^0 in the data and MC, $\frac{\sigma_{\rm data}}{\sigma_{\rm mc}}$, where $\sigma_{\rm data}$ is the resolution of Ξ_c^0 for data and $\sigma_{\rm mc}$ is that for MC. An additional cut of $2.64\,{\rm GeV}/c^2 < M(\Xi_c^0\pi^+) < 2.65\,{\rm GeV}/c^2$ is applied to select the $\Xi_c(2645)^+$ region only. $\frac{\sigma_{\rm data}}{\sigma_{\rm mc}}$ is 0.96 ± 0.03, 1.03 ± 0.07, and 1.07 ± 0.03 for the $\Xi^-\pi^+$, $\Lambda K^-\pi^+$, and $pK^-K^-\pi^+$ decay modes, respectively. We assign the systematic uncertainty conservatively by increasing the mass resolution by 7%, which is the largest deviation of the $\frac{\sigma_{\rm data}}{\sigma_{\rm mc}}$ from unity, for all the decay modes. The resulting width is 2.5 ± 0.2 MeV/c^2. The difference of 0.1 MeV/c^2 with respect to the default measurement is included as a systematic uncertainty. We use alternative x_p ranges of $0.35 < x_p < 1.0$ and $0.55 < x_p < 1.0$ and extract the width of 2.6 ± 0.2 MeV/c^2 for the former case and 2.8 ± 0.2 MeV/c^2 for the latter. The largest difference of 0.2 MeV/c^2 with respect to the default measurement is included as a systematic uncertainty. By adding all the systematic uncertainties in quadrature, the total systematic uncertainty for the width measurement is estimated to be 0.4 MeV/c^2.

C. Search for doubly charmed baryons in the $\Xi_c^0\pi^+(\pi^+)$ final state

To obtain the relative yields of the Ξ_{cc}, $\varepsilon^i_{\Xi_{cc}}$ and $\varepsilon^i_{\Xi_c(2645^+)}$ are evaluated using MC, and the efficiency $\varepsilon^i_{\Xi_{cc}}$ is obtained as a function of the Ξ_{cc} mass. $N^i_{\Xi_c(2645)^+}$ and $\varepsilon^i_{\Xi_c(2645^+)}$ are summarized in Table IV, while $\varepsilon^i_{\Xi^+_{cc}}$ as a function of Ξ_{cc} mass is shown in Fig. 5. As an example, the relative yield ratio of the Ξ^+_{cc} with a mass of 3.6 GeV/c^2 is $N^{\Xi^-\pi^+}_{\Xi^+_{cc}} : N^{\Lambda K^-\pi^+}_{\Xi^+_{cc}} : N^{pK^-K^-\pi^+}_{\Xi^+_{cc}} = 1 : 1.15 : 0.84$.

Figures 6 and 7(a)–(c) show the $M(\Xi_c^0\pi^+(\pi^+))$ distribution in the Ξ_{cc} search region with all the selection cuts applied, overlaid with the MC expectation for the Ξ_{cc} at the mass of $3.60\,{\rm GeV}/c^2$ with $\sigma(e^+e^- \to \Xi_{cc}^{+(+)}X)$ of 500 fb and both $\mathcal{B}(\Xi_{cc}^{+(+)} \to \Xi_c^0\pi^+(\pi^+))$ and $\mathcal{B}(\Xi_c^0 \to \Xi^-\pi^+)$ of 5%. The relative yields of signal MC for each decay mode are based on $N^i_{\Xi_{cc}}$.

A simultaneous UML fit, with the relative Ξ_{cc} yields constrained as discussed earlier, is applied to evaluate the statistical significance of the Ξ_{cc}. The signal PDF is described with MC events generated for each decay mode and with the Ξ_{cc} mass generated in the search region with a 1 MeV/c^2 step. The mass resolution is 2.7–4.2 MeV/c^2, depending on the mass of the Ξ_{cc}. The background PDF is modeled as a third-order polynomial. The highest significance is 3.2σ for the mass around 3.553 GeV/c^2 in the $M(\Xi_c^0\pi^+)$. We perform a pseudoexperiment test to evaluate the probability of observing a peak with such a statistical significance. A smooth mass distribution based on data is generated and the significance is evaluated in the entire search region. The probability to observe a peak with a significance higher than 3.2σ in one pseudoexperiment is 26%. Therefore, the statistical significance of 3.2σ is insufficient to claim evidence of the Ξ^+_{cc}.

TABLE IV. $\Xi_c(2645)^+$ yields and efficiencies used for estimation of the relative Ξ_{cc} yields.

Decay mode	$N_{\Xi_c(2645)^+}$	$\varepsilon_{\Xi_c(2645)^+}$
$\Xi^-\pi^+$	1298 ± 51	0.0748 ± 0.0002
$\Lambda K^-\pi^+$	1444 ± 58	0.0977 ± 0.0003
$pK^-K^-\pi^+$	974 ± 47	0.1920 ± 0.0005

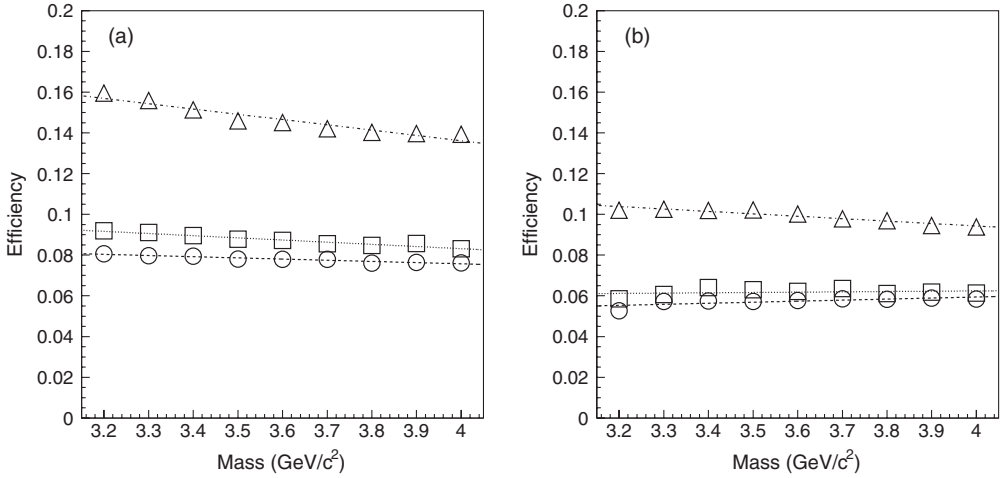

FIG. 5. Reconstruction efficiencies for the Ξ_{cc} as a function of the Ξ_{cc} mass for (a) Ξ_{cc}^{+}, (b) Ξ_{cc}^{++}. Circles, square, and triangle points are for $\Xi_c^0 \to \Xi^-\pi^+$, $\Lambda K^-\pi^+$, and $pK^-K^-\pi^+$, respectively. The lines are the result of the fit with a linear function.

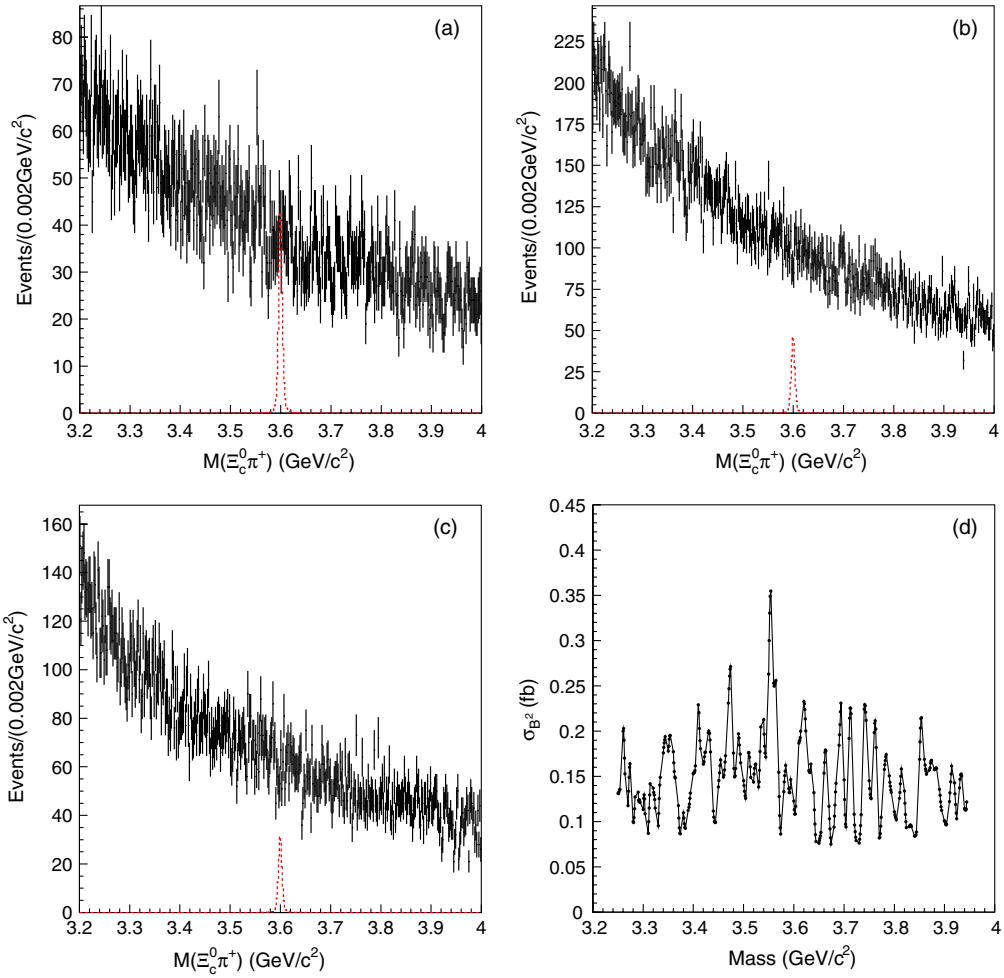

FIG. 6 (color online). (a)–(c): $M(\Xi_c^0\pi^+)$ distribution in the Ξ_{cc}^{+} search region for $\Xi_c^0 \to$ (a) $\Xi^-\pi^+$, (b) $\Lambda K^-\pi^+$, (c) $pK^-K^-\pi^+$. The vertical error bars are from data. The dashed histograms are from signal MC. (d): 95% C.L. upper limit of the σ_{B^2} for Ξ_{cc}^{+} as a function of the mass with a 1 MeV/c^2 step.

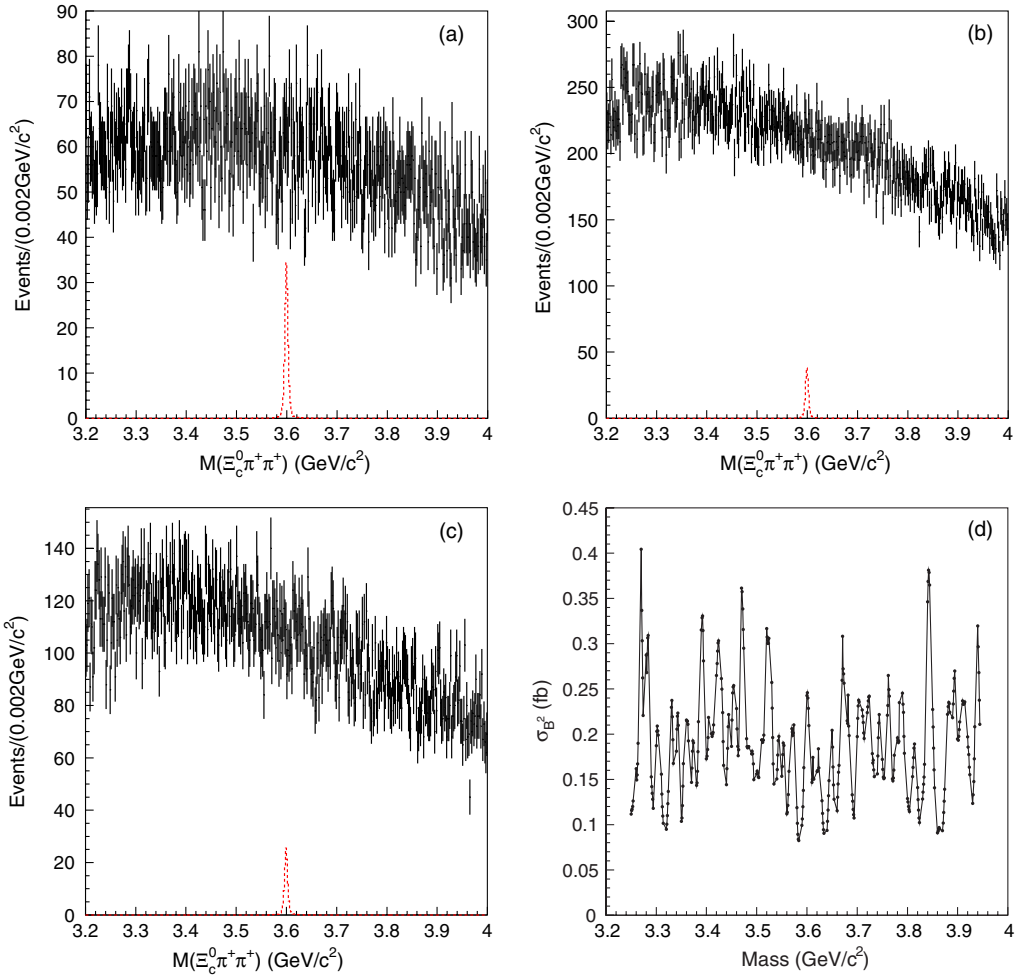

FIG. 7 (color online). (a)–(c): $M(\Xi_c^0\pi^+\pi^+)$ distribution in the Ξ_{cc}^{++} search region for $\Xi_c^0 \to$ (a) $\Xi^-\pi^+$, (b) $\Lambda K^-\pi^+$, (c) $pK^-K^-\pi^+$. The vertical error bars are from data. The dashed histograms are from signal MC. (d): 95% C.L. upper limit of the $\sigma_{\mathcal{B}^2}$ for Ξ_{cc}^{++} as a function of the mass with a 1 MeV/c^2 step.

The 95% C.L. upper limit for the product of the cross section and branching fractions produced with $0.45 < x_p < 1.0$ condition,

$$\sigma_{\mathcal{B}^2} \equiv \sigma(e^+e^- \to \Xi_{cc}^{+(+)}X) \times \mathcal{B}(\Xi_{cc}^{+(+)} \to \Xi_c^0\pi^+(\pi^+)) \times \mathcal{B}(\Xi_c^0 \to \Xi^-\pi^+) = \frac{N_{\rm sig}}{2L \times \varepsilon_{\Xi_{cc}}^{\Xi^-\pi^+}\left(1 + \frac{N_{\Xi_{cc}}^{\Lambda K^-\pi^+}}{N_{\Xi_{cc}}^{\Xi^-\pi^+}} + \frac{N_{\Xi_{cc}}^{pK^-K^-\pi^+}}{N_{\Xi_{cc}}^{\Xi^-\pi^+}}\right)},$$

is evaluated with the same method as in Sec. III B. In addition to the sources from the study with the Λ_c^+, two others are included here. The systematic uncertainty from the Λ reconstruction efficiency is estimated to be 3% using the yield of the $B^+ \to \Lambda\bar{\Lambda}K^+$ with and without the requirement using decay vertex information. The systematic uncertainties related to $N^i_{\Xi_c(2645)^+}$ are taken from their statistical errors. The systematic uncertainties are summarized in the fourth column in Table II. Figures 6 and 7(d) show $\sigma_{\mathcal{B}^2}$ for the $\Xi_{cc}^{+(+)}$ as a function of the mass with a 1 MeV/c^2 step. The 95% C.L. upper limit on $\sigma_{\mathcal{B}^2}$ is 0.076–0.35 fb for the Ξ_{cc}^+ and 0.082–0.40 fb for the Ξ_{cc}^{++}.

V. CONCLUSION

We have presented a search for doubly charmed baryons and a study of the charmed strange baryons $\Xi_c(3055)^+$, $\Xi_c(3123)^+$ and $\Xi_c(2645)^+$ using the full data sample (980 fb^{-1}) collected with the Belle detector. The search for doubly charmed baryons is an improved study of our previous work [2]. We use about two times statistics of previous work and several additional decay modes that were not studied in the previous work.

We search for the Ξ_{cc} in the $\Lambda_c^+K^-\pi^+(\pi^+)$ and $\Xi_c^0\pi^+(\pi^+)$ final states. The Λ_c^+ is reconstructed from the $pK^-\pi^+$ and pK_S^0 decay modes. We do not find any significant Ξ_{cc} signal and set a 95% C.L. upper limit on

$\sigma(e^+e^- \to \Xi_{cc}^{+(+)}X) \times \mathcal{B}(\Xi_{cc}^{+(+)} \to \Lambda_c^+ K^-\pi^+(\pi^+))$ with the scaled momentum $0.5 < x_p < 1.0$: 4.1–25.0 fb for Ξ_{cc}^+ and 2.5–26.5 fb for Ξ_{cc}^{++}. We also search for the Ξ_{cc} in the $\Xi_c^0\pi^+(\pi^+)$ final state. The Ξ_c^0 is reconstructed from the $\Xi^-\pi^+$, $\Lambda K^-\pi^+$, and $pK^-K^-\pi^+$ decay modes. We do not find any significant Ξ_{cc} signal and set a 95% C.L. upper limit on $\sigma(e^+e^- \to \Xi_{cc}^{+(+)}X) \times \mathcal{B}(\Xi_{cc}^{+(+)} \to \Xi_c^0\pi^+(\pi^+)) \times \mathcal{B}(\Xi_c^0 \to \Xi^-\pi^+)$ with the scaled momentum $0.45 < x_p < 1.0$: 0.076–0.35 fb for the Ξ_{cc}^+ and 0.082–0.40 fb for the Ξ_{cc}^{++}. When we compare these values with the measurements by *BABAR*, we should note several things. We should multiply our result by two as written in Sec. III. For the final states with Λ_c^+, their upper limit is for the product of the cross section, $\mathcal{B}(\Xi_{cc}^{+(+)} \to \Lambda_c^+ K^-\pi^+(\pi^+))$ and $\mathcal{B}(\Lambda_c^+ \to pK^-\pi^+)$. The values presented in Ref. [34] are the highest upper limits in the search region, which can be compared with our highest values. After taking into account these points, we find our limits represent improvements by about a factor two for the final states with Λ_c^+ and a factor of four for the final states with Ξ_c^0.

If we assume $\mathcal{B}(\Xi_{cc}^{+(+)} \to \Lambda_c^+ K^-\pi^+(\pi^+))$, $\mathcal{B}(\Xi_{cc}^{+(+)} \to \Xi_c^0\pi^+(\pi^+))$, and $\mathcal{B}(\Xi_c^0 \to \Xi^-\pi^+)$ to be 5%, which is equal to the $\mathcal{B}(\Lambda_c^+ \to pK^-\pi^+)$, the upper limits on the $\sigma(e^+e^- \to \Xi_{cc}^+X)$ are 82–500 fb (Ξ_{cc}^+) and 50–530 fb (Ξ_{cc}^{++}) for the decay mode with the Λ_c^+ and 30–140 fb (Ξ_{cc}^+) and 33–160 fb (Ξ_{cc}^{++}) for the decay mode with the Ξ_c^0. These values are comparable to some of the theoretical predictions [28,29].

We have searched for the $\Xi_c(3055)^+$ and $\Xi_c(3123)^+$ in the $\Lambda_c^+K^-\pi^+$ decays through intermediate $\Sigma_c(2455)^{++}$ or $\Sigma_c(2520)^{++}$ states. We observe the $\Xi_c(3055)^+$ with a significance of 6.6σ, including systematic uncertainty. The mass and width are measured to be $3058.1 \pm 1.0(\text{stat}) \pm 2.1(\text{sys})$ MeV/c^2 and $9.7 \pm 3.4(\text{stat}) \pm 3.3(\text{sys})$ MeV/c^2, respectively. We do not observe any significant signal corresponding to the $\Xi_c(3123)^+$.

The first measurement of the width of the $\Xi_c(2645)^+$ has been also performed, yielding $2.6 \pm 0.2(\text{stat}) \pm 0.4(\text{sys})$ MeV/c^2.

ACKNOWLEDGMENTS

We thank the KEKB group for the excellent operation of the accelerator; the KEK cryogenics group for the efficient operation of the solenoid; and the KEK computer group, the National Institute of Informatics, and the PNNL/EMSL computing group for valuable computing and SINET4 network support. We acknowledge support from the Ministry of Education, Culture, Sports, Science, and Technology (MEXT) of Japan, the Japan Society for the Promotion of Science (JSPS), and the Tau-Lepton Physics Research Center of Nagoya University; the Australian Research Council and the Australian Department of Industry, Innovation, Science and Research; Austrian Science Fund under Grant No. P 22742-N16; the National Natural Science Foundation of China under Contracts No. 10575109, No. 10775142, No. 10825524, No. 10875115, No. 10935008, and No. 11175187; the Ministry of Education, Youth and Sports of the Czech Republic under Contract No. MSM0021620859; the Carl Zeiss Foundation, the Deutsche Forschungsgemeinschaft and the VolkswagenStiftung; the Department of Science and Technology of India; the Istituto Nazionale di Fisica Nucleare of Italy; The WCU program of the Ministry Education Science and Technology, National Research Foundation of Korea Grants No. 2011-0029457, No. 2012-0008143, No. 2012R1A1A2008330, No. 2013R1A1A3007772, BRL program under NRF Grant No. KRF-2011-0020333, BK21 Plus program, and GSDC of the Korea Institute of Science and Technology Information; the Polish Ministry of Science and Higher Education and the National Science Center; the Ministry of Education and Science of the Russian Federation and the Russian Federal Agency for Atomic Energy; the Slovenian Research Agency; the Basque Foundation for Science (IKERBASQUE) and the UPV/EHU under program UFI 11/55; the Swiss National Science Foundation; the National Science Council and the Ministry of Education of Taiwan; and the U.S. Department of Energy and the National Science Foundation. This work is supported by a Grant-in-Aid from MEXT for Science Research in a Priority Area ("New Development of Flavor Physics"), from JSPS for Creative Scientific Research ("Evolution of Tau-lepton Physics"), and Grant-in-Aid for Scientific Research on Innovative Areas "Elucidation of New Hadrons with a Variety of Flavors".

[1] R. Mizuk *et al.* (Belle Collaboration), Phys. Rev. Lett. **94**, 122002 (2005).
[2] R. Chistov *et al.* (Belle Collaboration), Phys. Rev. Lett. **97**, 162001 (2006).
[3] B. Aubert *et al.* (*BABAR* Collaboration), Phys. Rev. Lett. **97**, 232001 (2006).
[4] B. Aubert *et al.* (*BABAR* Collaboration), Phys. Rev. Lett. **98**, 012001 (2007).
[5] K. Abe *et al.* (Belle Collaboration), Phys. Rev. Lett. **98**, 262001 (2007).
[6] B. Aubert *et al.* (*BABAR* Collaboration), Phys. Rev. D **77**, 012002 (2008).

[7] E. Solovieva, R. Chistov, I. Adachi, H. Aihara, K. Arinstein, T. Aushev, A. M. Bakich, and V. Balagura *et al.*, Phys. Lett. B **672**, 1 (2009).

[8] T. Lesiak *et al.* (Belle Collaboration), Phys. Lett. B **665**, 9 (2008).

[9] J. Beringer *et al.* (Particle Data Group Collaboration), Phys. Rev. D **86**, 010001 (2012).

[10] R. Roncaglia, D. B. Lichtenberg, and E. Predazzi, Phys. Rev. D **52**, 1722 (1995).

[11] D. Ebert, R. N. Faustov, V. O. Galkin, A. P. Martynenko, and V. A. Saleev, Z. Phys. C **76**, 111 (1997).

[12] B. Silvestre-Brac, Prog. Part. Nucl. Phys. **36**, 263 (1996).

[13] S.-P. Tong, Y.-B. Ding, X.-H. Guo, H.-Y. Jin, X.-Q. Li, P.-N. Shen, and R. Zhang, Phys. Rev. D **62**, 054024 (2000).

[14] S. M. Gerasyuta and D. V. Ivanov, Nuovo Cimento A **112**, 261 (1999).

[15] C. Itoh, T. Minamikawa, K. Miura, and T. Watanabe, Phys. Rev. D **61**, 057502 (2000).

[16] V. V. Kiselev and A. K. Likhoded, Usp. Fiz. Nauk **172**, 497 (2002) [Phys. Usp. **45**, 455 (2002)].

[17] I. M. Narodetskii and M. A. Trusov, arXiv:hep-ph/0204320.

[18] D. Ebert, R. N. Faustov, V. O. Galkin, and A. P. Martynenko, Phys. Rev. D **66**, 014008 (2002).

[19] J. Vijande, H. Garcilazo, A. Valcarce, and F. Fernandez, Phys. Rev. D **70**, 054022 (2004).

[20] S. Migura, D. Merten, B. Metsch, and H.-R. Petry, Eur. Phys. J. A **28**, 41 (2006).

[21] C. Albertus, E. Hernandez, J. Nieves, and J. M. Verde-Velasco, Eur. Phys. J. A **32**, 183 (2007); C. Albertus, E. Hernandez, J. Nieves, and J. M. Verde-Velasco, Eur. Phys. J. A **36**, 119(E) (2008).

[22] W. Roberts and M. Pervin, Int. J. Mod. Phys. A **23**, 2817 (2008).

[23] R. Lewis, N. Mathur, and R. M. Woloshyn, Phys. Rev. D **64**, 094509 (2001).

[24] H. Na and S. Gottlieb, *Proc. Sci.*, LATTICE (**2008**) 119 [arXiv:0812.1235].

[25] L. Liu, H.-W. Lin, K. Orginos, and A. Walker-Loud, Phys. Rev. D **81**, 094505 (2010).

[26] Y. Namekawa, (PACS-CS Collaboration) *Proc. Sci.*, LATTICE (**2012**) 139 [arXiv:1212.0073].

[27] C. Alexandrou, J. Carbonell, D. Christaras, V. Drach, M. Gravina, and M. Papinutto, Phys. Rev. D **86**, 114501 (2012).

[28] V. V. Kiselev, A. K. Likhoded, and M. V. Shevlyagin, Phys. Lett. B **332**, 411 (1994).

[29] J. P. Ma and Z. G. Si, Phys. Lett. B **568**, 135 (2003).

[30] V. V. Braguta, V. V. Kiselev, and A. E. Chalov, Yad. Fiz. **65**, 1575 (2002) [Phys. At. Nucl. **65** 1537 (2002)].

[31] M. Mattson *et al.* (SELEX Collaboration), Phys. Rev. Lett. **89**, 112001 (2002).

[32] A. Ocherashvili *et al.* (SELEX Collaboration), Phys. Lett. B **628**, 18 (2005).

[33] S. P. Ratti, Nucl. Phys. B, Proc. Suppl. **115**, 33 (2003).

[34] B. Aubert *et al.* (*BABAR* Collaboration), Phys. Rev. D **74**, 011103 (2006).

[35] R. Aaij *et al.* (LHCb Collaboration), J. High Energy Phys. 12 (2013) 090.

[36] L. Gibbons *et al.* (CLEO Collaboration), Phys. Rev. Lett. **77**, 810 (1996).

[37] S. Kurokawa and E. Kikutani, Nucl. Instrum. Methods Phys. Res., Sect. A **499**, 1 (2003), and other papers included in this volume; T. Abe *et al.*, Prog. Theor. Exp. Phys. (**2013**) 03A001 and following articles up to 03A011.

[38] A. Abashian *et al.* (Belle Collaboration), Nucl. Instrum. Methods Phys. Res., Sect. A **479**, 117 (2002); also see detector section in J. Brodzicka *et al.*, Prog. Theor. Exp. Phys. (**2012**), 04D001.

[39] Z.Natkaniec *et al.* (Belle SVD2 Group), Nucl. Instrum. Methods Phys. Res., Sect. A **560**, 1 (2006).

[40] K. Hanagaki, H. Kakuno, H. Ikeda, T. Iijima, and T. Tsukamoto, Nucl. Instrum. Methods Phys. Res., Sect. A **485**, 490 (2002).

[41] D. J. Lange, Nucl. Instrum. Methods Phys. Res., Sect. A **462**, 152 (2001).

[42] T. Sjostrand, Comput. Phys. Commun. **82**, 74 (1994).

[43] E. Barberio and Z. Was, Comput. Phys. Commun. **79**, 291 (1994).

[44] R. Brun *et al.*, GEANT3.21, CERN Report No. DD/EE/84-1, 1984.

[45] Throughout this paper, the inclusion of the charge-conjugate decay mode is implied unless otherwise stated.

[46] K. Sumisawa *et al.* (Belle Collaboration), Phys. Rev. Lett. **95**, 061801 (2005).

[47] B. Aubert *et al.* (*BABAR* Collaboration), Phys. Rev. D **75**, 012003 (2007).

[48] K. Abe *et al.* (Belle Collaboration), Phys. Rev. D **65**, 091103 (2002).